The spherical involute bevel gear: Its geometry, kinematic behavior and standardization

Article *in* Journal of Mechanical Science and Technology · April 2011

DOI: 10.1007/s12206-011-0145-1

2 authors, including:

Nogill Park
Pusan National University
46 PUBLICATIONS **214** CITATIONS

SEE PROFILE

Springer

KSME

Journal of Mechanical Science and Technology 25 (4) (2011) 1023~1034
www.springerlink.com/content/1738-494x
DOI 10.1007/s12206-011-0145-1

The spherical involute bevel gear: its geometry, kinematic behavior and standardization †

Noh Gill Park and Hyoung Woo Lee*

School of Mechanical Engineering Pusan National University, Korea

(Manuscript Received December 11, 2009; Revised February 7, 2011; Accepted February 14, 2011)

Abstract

Bevel gear processing has diversified based on constant technical developments in forging, CNC cutting and hob design. Standardization of bevel gears is in higher demand than ever for different bevel gear systems that have different shapes and forms according to processing methods. With advantages such as excellent compatibility and the ability to absorb assembly errors well, the involute gear is referred to as the spherical involute tooth profile in bevel gear systems. This paper explains the geometrical characteristics and kinematic behavior of spherical involute gears. A spherical involute function is derived to effectively represent tooth profiles, and a common basic rack is developed using the equation of meshing to generate spherical involute gears. This study also analyzes the general characteristics of spherical involute gears and discusses the issue of bevel-gear standardization.

Keywords: Spherical involute gears; Standardization of bevel gears; Tooth profiles; Compatibility

1. Introduction

A bevel gear is a gear element that efficiently transfers power and motion at an intersection of multiple axes. Some bevel gears have tooth profiles with benefits similar to those found in involute-type gears most frequently used in parallel-axis gear systems. However, processing methods for such tooth profiles are not commercially available and researchers have conducted few studies on the issue. Since commercial bevel gears have different tooth profiles depending on the processing machine, it would not be an overstatement to say that a standardized tooth profile does not exist. Therefore, a number of restrictions exist in the use of bevel gears. Forging and CNC-processing technologies have recently shown progress and are now often used in bevel gear processing. Even though forged gears are inferior to cut gears in terms of precision, the gap is gradually narrowing. While CNC processing yields the most precise output, it is rarely used in mass manufacturing—due to high processing costs—and only partially used in finishing-process stages. However, both processing techniques require standardized gear-tooth profiles. Accordingly, the field needs to establish a basis for standardizing bevel gears by promoting studies on spherical involute gears and their numerous advantages.

Although spherical involute gears have superior bevel gar-tooth profiles, researchers have scarcely studied their geometrical characteristics and kinematic behavior. The spherical involute gear configuration proposed by Tsai and Chin [1] offered an approximate involute tooth profile. Mark [2] mathematically derived the transmission error of the spiral bevel gear, and his paper introduced the kinematic relationship of a complete involute bevel gear pair. He assumed that two base cones perform a rolling contact motion with the disk of action as the common contact surface. In 1994, Al-Daccak, et al. [3] benchmarked a complete spherical involute tooth profile in a solid modeling attempt of a non-standardized bevel gear and numerically examined its geometrical characteristics.

This paper will present the advantages of spherical and cylindrical involute gears and establish fundamental theories on standardized bevel gear design by explaining its unique geometrical characteristics. To do so, a spherical involute function is introduced to define the spherical involute bevel gear configuration. The spherical involute function takes a generalized form of the involute function of cylindrical involute gears and can be easily used in calculating bevel gear-tooth thickness. Using the equation of meshing [4], a common basic rack that generates a known spherical involute gear is mathematically derived. Cylindrical involute gears are already standardized and widely used throughout the industry. Standardization of bevel gears must be attempted to expand the usage of bevel gear systems. This paper proposes a standard bevel gear that

† This paper was recommended for publication in revised form by Associate Editor Eung-Soo Shin

* Corresponding author. Tel.: +82 51 510 2598, Fax.: +82 51 581 2964
E-mail address: leehwoo@pusan.ac.kr

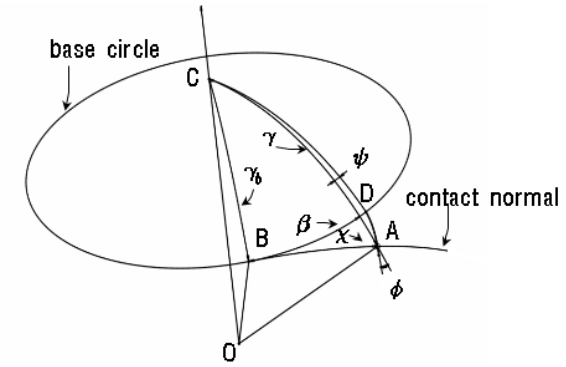

Fig. 1. Spherical involute curve.

corresponds to a standard spur gear. A tooth profile of a crown rack for generating the standard bevel gear is proposed, and the tooth-profile curve is calculated using the equation of meshing. Also, the tooth-profile curve characteristics of the proposed standard bevel gear's fillet part are examined, and the limit of teeth number for preventing undercutting is calculated.

2. Spherical involute function

The involute function is a means of mathematically defining the tooth-profile curve of a spur gear. Whereas a tooth-profile curve generally involves complex mathematical procedures, the involute function facilitates its manipulation. Since it is a widely known fact that the bevel gear system is a generalized configuration of the parallel-axis gear system, it is believed that the geometrical procedures of the tooth-profile curve in a complex bevel gear system can be simplified by deriving the spherical involute function, which is a generalized form of the cylindrical involute function.

Unless specified otherwise, bevel gear configuration will be expressed on a transverse sphere in this paper. A transverse sphere refers to a reference sphere with a radius of ξ, and two axes intersect at the center of the sphere. When it converges to a cylindrical gear, it becomes a transverse plane perpendicular to the gear axis. Fig. 1 displays the spherical involute tooth profile.

The edge of the base cone is referred to as the base circle, the center of which is represented by point C on the transvers sphere. The trajectory of point A at the tip of arc $\widehat{AB}$ is the spherical involute curve $\widehat{DA}$. The tooth-profile angle ϕ at an arbitrary point A on the curve is defined by the angle between the tangent line of the curve and arc $\widehat{AC}$. Curve $\widehat{DA}$ and arc $\widehat{AB}$ are always perpendicular. Therefore, $\widehat{BC}$ and $\widehat{AB}$ are perpendicular, and the spherical triangle ΔABC is a right triangle. The relationships between the angles and the sides of a spherical triangle are different from those of a plane triangle (Refer to Appendix 1). In Fig. 1, the relationships among $\gamma, \gamma_b, \chi, \phi$ and β are as follows:

$$\cos\gamma = \cos\gamma_b \cos\chi \tag{1}$$

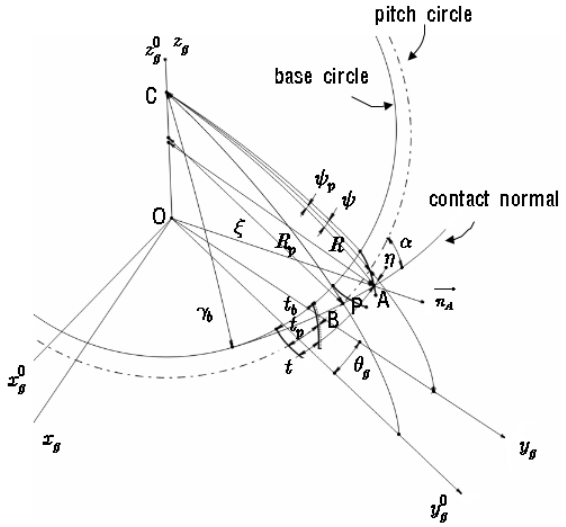

Fig. 2. Basic parameters of spherical involute gear.

$$\sin\phi = \frac{\tan\chi}{\tan\gamma} \tag{2}$$

$$\cos\beta = \frac{\tan\gamma_b}{\tan\gamma} \tag{3}$$

where γ, γ_b, χ are angle-parameters representing $\angle COA$, $\angle COB, \angle BOA$, respectively and azmith angle β is the angle between arc $\widehat{BC}$ and $\widehat{AC}$. Eliminating the angle X from Eqs. (1) and (2), we obtain

$$\sin\gamma_b = \cos\phi \sin\gamma. \tag{4}$$

The spherical involute function refers to angle Ψ between $\widehat{AC}$ and $\widehat{CD}$ in Fig. 1. Since the lengths of $\widehat{BD}$ and $\widehat{AB}$ are identical,

$$X = (\beta + \psi)\sin\gamma_b. \tag{5}$$

Expressing it in terms of ψ gives

$$\psi = \frac{X}{\sin\gamma_b} - \beta. \tag{6}$$

In Eq. (6), the spherical involute function can be written as a function of ϕ and base-cone angle γ_b.

$$\psi = \frac{1}{\sin\gamma_b}\tan^{-1}\left(\frac{\sin\gamma_b \sin\phi}{\sqrt{\cos^2\phi - \sin^2\gamma_b}}\right) - \cos^{-1}\left(\frac{\sqrt{\cos^2\phi - \sin^2\gamma_b}}{\cos\gamma_b}\right) \tag{7}$$

Since $\gamma_b -> 0$ if $\xi -> \infty$, Eq. (7) converges to $\psi = \tan\phi - \phi$. From this, it can be confirmed that the spherical involute tooth profile is a generalized configuration of the cylindrical involute tooth profile. ψ can be expressed with cone angle γ instead of ϕ. Applying Eq. (3) and rearranging,

we obtain

$$\psi = \frac{1}{\sin\gamma_b}\cos^{-1}\left(\frac{\cos\gamma}{\cos\gamma_b}\right) - \cos^{-1}\left(\frac{\tan\gamma_b}{\tan\gamma}\right). \quad (8)$$

Fig. 2 depicts the basic parameters of a spherical involute gear.

The gear's pitch circle is used as a reference for defining its tooth profile. A pitch point P is the intersection of a pitch circle and the center line of axis, and the common normal of the tooth-contact point passes through the pitch point. When the tooth-profile curve passes through a pitch point, the tooth-profile curve angle at the point is referred to as the gear pressure angle a_g. In a standard gear, the gear pressure angle and the rack (or tool) pressure angle a is identical. The relationship among a, γ_b and the pitch cone angle $\gamma_p(\angle COP)$ in Fig. 2 is obtained from Eq. (4).

$$\sin\gamma_b = \cos\alpha\sin\gamma_p \quad (9)$$

The relationship between the tooth thickness on the pitch circle, space width and backlash B is

$$t_p = \frac{p - B}{2} \quad (10)$$

where p is the standard pitch of gear. Accordingly, tooth thickness t at an arbitrary point A on the tooth-profile curve is

$$t = R\left(\frac{t_p}{R_p} + 2\psi_p - 2\psi\right) \quad (11)$$

where $R = A\sin\gamma$ and $R_P = A\sin\gamma_p$. ψ is obtained from Eq. (7) or (8), and ψ_p is obtained by substituting $\phi = a$ into Eq. (7) or $\gamma = \gamma_p$ into Eq. (8).

$$\psi_b = \frac{1}{\sin\gamma_b}\tan^{-1}\left(\frac{\sin\gamma_b\sin\alpha}{\sqrt{\cos^2\alpha - \sin^2\gamma_b}}\right) - \cos^{-1}\left(\frac{\sqrt{\cos^2\alpha - \sin^2\gamma_b}}{\cos\gamma_b}\right) \quad (12)$$

Since the base circle's tooth thickness t_b is the tooth thickness when $\gamma = \gamma_b$ in Eq. (11), at which point $\psi = 0$, t_b becomes

$$t_b = R_b\left(\frac{t_p}{R_p} + 2\psi_p\right) \quad (13)$$

where $R_b = A\sin\gamma_b$. A module m determines the tooth size. The bevel gear's module is defined in the same way as that of a spur gear. If the pitch circle diameter and the number of teeth are given to D_P and Z,

$$m = \frac{D_p}{z}. \quad (14)$$

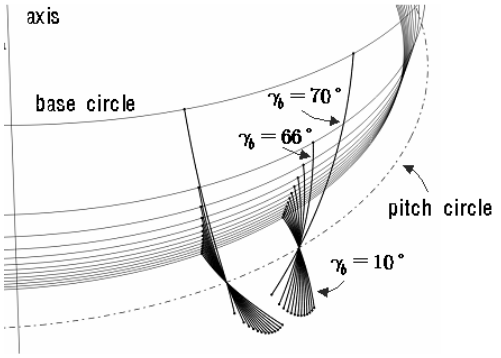

Fig. 3. Teeth profiles of spherical involute gear with $\gamma_b = 10° \sim 70°$.

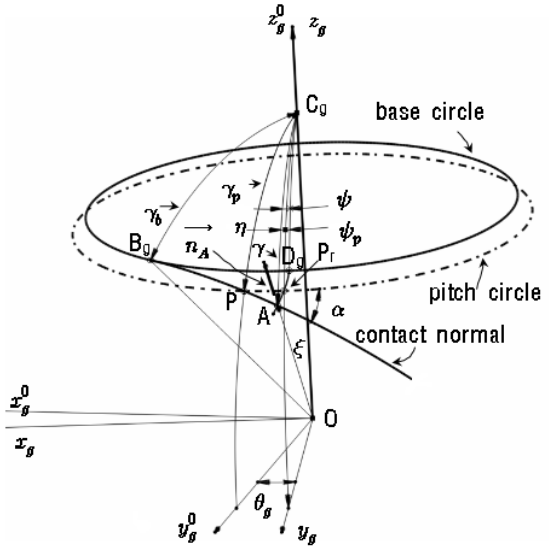

Fig. 4. The spherical involute tooth-profile and the coordinate systems.

Spherical involute tooth profiles for different base-cone angles in a single module are depicted in Fig. 3, which displays tooth-profile curves with addendum angle γ_a at m/ξ=0.1, m=3.0, $\alpha = 20°$, $Z = 20$, and $\gamma_b = 10° \sim 70°$.

The tooth-tip circle radius R_t becomes $\xi\sin(\gamma_p + \gamma_a)$, which is reduced as γ_b increases. When γ_b reaches its maximum of 70°, R_t is smaller than the pitch-circle radius R_P. t_b increases in proportion to γ_b. Since a bevel gear has a thick t_b, it can be learned that it has greater strength than a spur gear.

The spherical involute tooth-profile curve can be expressed on the gear fixed coordinate system C_g. In C_g, z_g is the gear rotational axis and y_g axis is directed toward the intersection P_r of the tooth-profile curve and the tooth-pitch circle, as shown in Fig. 4.

Therefore,

$$\overrightarrow{OA} = \xi\overrightarrow{n_A} \quad (15)$$

$$\overrightarrow{n_A} = \sin\gamma\sin\eta\overrightarrow{i_g} + \sin\gamma\cos\eta\overrightarrow{j_g} + \cos\gamma\overrightarrow{k_g} \quad (16)$$

$$\eta = \psi - \psi_p \quad (17)$$

where η, γ are the angles of $\widehat{C_g A}$, $\widehat{C_g P_r}$, respectively. Gear's rigid body motion can be defined by the relationship between the space-fixed gear reference coordinate system ${C_g}^0$ and C_g. C_g is constructed by rotationally displacing ${C_g}^0$ in the positive direction by the gear's angular motion θ_g with ${z_g}^0$ as the reference axis.

3. Common crown rack

When the rack and its conjugate rack have an identical configuration, it is referred to as a common rack, which has two advantages. The first is that separate racks are not necessary for generating the two gears. Both gears can be cut with a single rack, reducing manufacturing costs. A greater advantage is that every gear cut with the common rack is compatible. For bevel gears available in the commercial market, two gears manufactured with different processing machines cannot be assembled. However, if a design methodology is established based on a common basic rack for bevel gear systems and corresponding manufacturing techniques are developed and distributed as in spur and helical gear systems, a single hob becomes sufficient, and every bevel gear generated with the hob becomes compatible. Undoubtedly, this will open paths for bevel gear standardization and play a significant role in making spherical involute gears as widely available as spur and helical involute gears.

A crown rack will be derived in this paper from the spherical involute tooth profile with a complete mathematical definition using the gear mesh equation. Examining the geometrical relationship between the involute gear and its common basic rack in a cylindrical gear system, we learn that the two are tooth profiles of the same type. The common rack is called as a linear rack in which the teeth have straight sides. If we assume a cylindrical involute gear with an infinite diameter while maintaining its module, its gear-tooth profile will converge into a linear rack. Therefore, we can conclude that a linear rack is one of asymptotic geometries of a cylindrical involute gear. If so, a crown rack is likely to be an asymptotic geometry of a spherical involute gear with a pitch-cone angle of $\pi/2$.

The concept of base circle is very useful, not only in gear design, but also for understanding kinematic behavior [5]. In cylindrical involute system, a base circle and a line of action come in contact at a single point, where they engage in uniform velocity motion and pure rolling contact. However, the base circle concept is mainly used to explain gear-pair motion and not the motion between gear and linear rack. This is because the base circle is not geometrically apparent in a linear rack. Nonetheless, since every geometry of a crown rack can be represented on a transverse sphere, it is evident that pitch and base circles exist on the transverse sphere. Also without doubt, assessing the base circle clearly is very important toward better understanding the kinematic behavior of bevel gears and the crown rack. Accordingly, the process of identifying the location of the base circle of crown rack will be explained subsequently. The spatial position of the circle of action will be first obtained using the gear mesh equation. Next, from the condition that the circle of action and the rack's base circle engage in rolling-contact motions around their respective fixed rotational axis, the position and configuration of the rack's base circle will be obtained. And also it will be mathematically verified that a crown rack is an asymptotic geometry of a spherical involute gear. Finally, the rack's tooth profile will be obtained from the definition of the spherical involute tooth curve based on the rack's base circle.

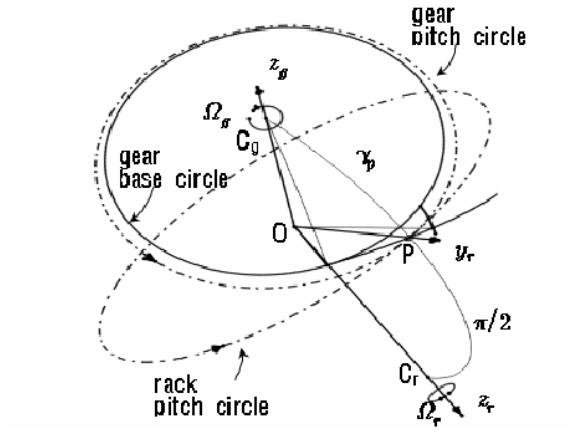

Fig. 5. Kinematic relation between pinion and basic rack.

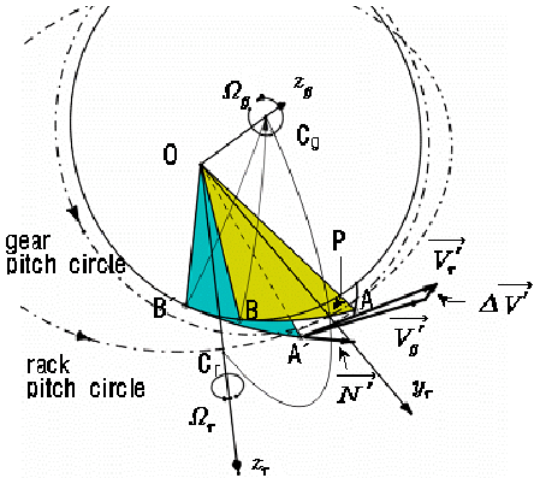

Fig. 6. Basic rack meshing gear.

3.1 Circle of action

Mark [3] explained that the trajectory of teeth contact point is a circle in a spherical involute gear system. In this paper the fact will be explained according to the equation of meshing [4]. Fig. 5 displays the kinematic relationship between a rack and gear that rotate around axes z_r and z_g, respectively, and two pitch circles in rolling-contact motions at pitch point P.

The rack's pitch circle is the edge of the pitch cone with a pitch-cone angle of $90°$. Therefore, the angle between rotational axes z_r and z_g becomes $\pi/2+\gamma_p$. From the condition that velocities on rack and gear pitch circles are equal,

the relationship between rotational velocities Ω_r and Ω_g becomes

$$\Omega_r = \Omega_g \sin\gamma_p . \tag{18}$$

In Fig. 6, if we assume that the spherical involute gear and crown rack come in contact at point A', arc $\widehat{A'B'}$ is a common normal of the gear and the rack, as shown in Fig. 1.

Moreover, for the gear and the rack to engage in proper motion, the following gear mesh equation must be satisfied.

$$\overrightarrow{N'} \bullet (\overrightarrow{V_g'} - \overrightarrow{V_r'}) = 0 \tag{19}$$

where $\overrightarrow{N'}$ is the tangent vector of tooth contact normal $\widehat{A'B'}$ at contact point A', and $\overrightarrow{V_g'}$ and $\overrightarrow{V_r'}$ are the velocities of gear and rack, respectively, at the same point. Therefore,

$$\overrightarrow{V_g'} = \overrightarrow{\Omega_g} \bullet \overrightarrow{OA'} \tag{20}$$

$$\overrightarrow{V_r'} = \overrightarrow{\Omega_r} \bullet \overrightarrow{OA'} . \tag{21}$$

Applying Eqs. (20) and (21) to Eq. (19), we obtain

$$\overrightarrow{N'} \bullet \{(\overrightarrow{\Omega_g} - \overrightarrow{\Omega_r}) \times \overrightarrow{OA'}\} = 0 . \tag{22}$$

Rewriting Eq. (22) using $\vec{a} \bullet (\vec{b} \times \vec{c}) = \vec{c} \bullet (\vec{a} \times \vec{b})$, we have

$$(\overrightarrow{\Omega_G} - \overrightarrow{\Omega_r}) \bullet (\overrightarrow{OA'} \times \overrightarrow{N'}) = 0 . \tag{23}$$

Meanwhile, since the crown rack and the gear rotate in the negative direction around z_r by Ω_r and in the positive direction around z_g by Ω_g, respectively,

$$\overrightarrow{\Omega_r} = -\Omega_r \overrightarrow{k_r} \tag{24}$$

$$\overrightarrow{\Omega_g} = \Omega_g \overrightarrow{k_g} . \tag{25}$$

Since the angle between z_r and z_g is $\pi/2 + \gamma_p$, from Eq. (18), we obtain

$$\overrightarrow{\Omega_g} - \overrightarrow{\Omega_r} = \Omega_g \cos\gamma_g \overrightarrow{j_r} \tag{26}$$

where $\overrightarrow{j_r}$ is unit vector of y_r direction.

In Eq. (26), the direction of $\overrightarrow{\Omega_g} - \overrightarrow{\Omega_r}$ is equal to that of $\overrightarrow{OP}$. Therefore, we can rewrite Eq. (23) as

$$\overrightarrow{OP} \bullet (\overrightarrow{OA'} \times \overrightarrow{N'}) = 0 . \tag{27}$$

In Fig. 6, circular sector $\Delta OA'B'$ is a plane. Since $\overrightarrow{N'}$ is tangent to arc $\widehat{A'B'}$ and $\overrightarrow{OA'}$ is on $\Delta OA'B'$, Eq. (27)'s $\overrightarrow{OA'} \times \overrightarrow{N'}$ term has the same direction as the plane $\Delta OA'B'$. Therefore, replacing $\overrightarrow{OA'} \times \overrightarrow{N'}$ with $\overrightarrow{OA'} \times \overrightarrow{OB'}$ does not alter the outcome of Eq. (27). In turn, from the mesh Eq. (19),

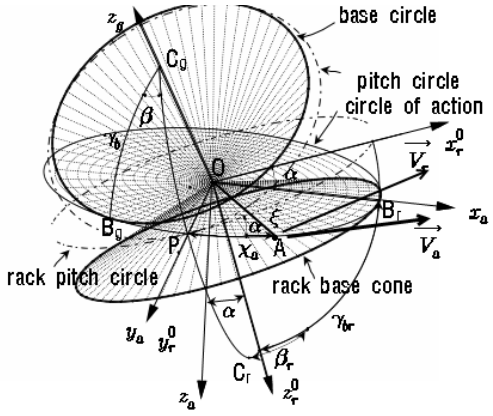

Fig. 7. Kinematic relationship between gear and basic rack.

we obtain the final relational equation

$$\overrightarrow{OP} \bullet (\overrightarrow{OA'} \times \overrightarrow{OB'}) = 0 . \tag{28}$$

Eq. (28) indicates that three different points A`,B`,P are on a single plane. Since pitch point P is a predefined fixed point in space in Fig. 6, $\widehat{A'B'}$ must pass through pitch point P. For the mesh equation to satisfy between gear and rack, tooth contact normal $\widehat{A'B'}$ has to displace to AB. Here, point A is the tooth-contact point of gear and rack, and point B is the tooth-contact point on the base circle. The trajectory of the tooth-contact point draws a circle that has a center point O and passes through P and B. From this, we learn that the tooth-contact point trajectory for spherical involute gear is circle.

Consequently, we can observe that the tooth-contact point A between gear and rack is on the circle of action fixed in space, as shown in Fig. 7, and the circle of action is tangent to the gear's base circle at point B_g.

If the gear engages in a uniform velocity circular motion at Ω_g around axis z_g, the trajectory of point A is also in a uniform velocity circular motion along the circle of action. The trajectory motion's rotational axis z_a is displaced by the amount of pressure angle α in the clockwise direction around the rack pitch circle's rotational axis $z_r{}^o$. And axis y_a of C_a is coincide with $y_r{}^0$. The angular velocity of tooth-contact point A is

$$\overrightarrow{\Omega_a} = -\Omega_a \overrightarrow{k_a} \tag{29}$$

$$\Omega_a = \Omega_g \sin\gamma_b \tag{30}$$

$$\overrightarrow{k_a} = -\sin\alpha \overrightarrow{i_r{}^0} + \cos\alpha \overrightarrow{k_r{}^0} . \tag{31}$$

3.2 Base circle of crown rack

As to the kinematic behavior of gear and rack and the concept of base circle using Fig. 7, the mechanism can be understood as base circles of gear and rack engaged in uniform velocity circular motions at Ω_g and Ω_r, respectively, the circle of action that links the two base circles being tangent to both circles and engaging in a uniform velocity circular mo-

tion at Ω_a. Here, the circle of action passes through pitch point P and is tangent with the base circles of the pinion and rack at fixed points B_g and B_r, respectively. Point B_r is the position of tooth-contact point A when the circle of action's velocity $\overrightarrow{V_a}$ and rack's velocity $\overrightarrow{V_r}$ coincide. Accordingly, the condition for obtaining $\overrightarrow{OB_r}$ is

$$\overrightarrow{V_a} = \overrightarrow{V_r} \tag{32}$$

where

$$\overrightarrow{V_a} = \overrightarrow{\Omega_a} \times \overrightarrow{OA} \tag{33}$$

$$\overrightarrow{V_r} = \overrightarrow{\Omega_r} \times \overrightarrow{OA} \tag{34}$$

$$\overrightarrow{OA} = \xi(\sin\chi_a \overrightarrow{i_a} + \cos\chi_a \overrightarrow{j_a}). \tag{35}$$

Applying Eqs. (24) and (29)-(31) to Eqs. (33)-(35), we obtain

$$\overrightarrow{V_a} = \Omega_a \xi(\cos\chi_a \overrightarrow{i_a} - \sin\chi_a \overrightarrow{j_a}) \tag{36}$$

$$\overrightarrow{V_r} = \Omega_r \xi(\cos\chi_a \cos\alpha \overrightarrow{i_a} - \sin\chi_a \cos a \overrightarrow{j_a} - \cos\chi_a \sin\alpha \overrightarrow{k_a} \tag{37}$$

Substituting Eqs. (36) and (37) into Eq. (32), we obtain $\cos\chi_a = 0$.

$$X_a = \frac{\pi}{2} \tag{38}$$

We now can substitute Eq. (38) into Eq. (35) to acquire the position of $\overrightarrow{OB_r}$.

$$\overrightarrow{OB_r} = \xi \overrightarrow{i_a} \tag{39}$$

Since the rack's base-cone angle is $\angle C_r O B_r$ in Fig. 7,

$$\gamma_{br} = \frac{\pi}{2} - a. \tag{40}$$

In Fig. 7, the azimuth angle becomes

$$\beta_r = \frac{\pi}{2}. \tag{41}$$

If the crown rack's tooth-profile curve is expected to be a specific form of the general spherical involute tooth-profile curve, the angular relationship between contact point B_r and pitch point P (Eqs. (38), (40) and (41)) must be identical to the result obtained from Eqs. (1), (3) and (9). Since the rack pitch-cone angle is $\pi/2$, substituting $\gamma_b = \pi/2$ into Eq. (9), we obtain $\gamma_b = \pi/2 - a$ .Substituting $\gamma_p = \pi/2$ and $\gamma_b = \pi/2 - \alpha$ into Eq. (1) yields $X = \pi/2$. Also, $\beta = \pi/2$ from Eq. (3). From these results, we can confirm that the crown rack's tooth-profile curve is a complete spherical involute tooth-profile curve with a pitch-cone angle of $\pi/2$ and base-cone

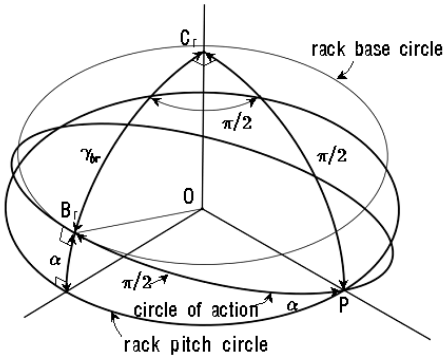

Fig. 8. Angles between B_r and P in the crown rack.

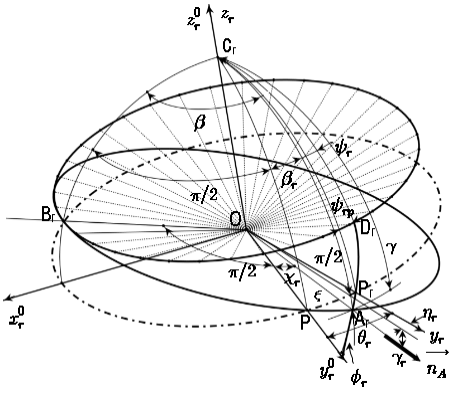

Fig. 9. Tooth profile of crown rack.

angle of $\pi/2 - \alpha$. The result is depicted in Fig. 8. Angles χ, γ, β between contact point B_r and pitch point P are all $\pi/2$.

The crown rack's tooth-profile curve is mathematically expressed with angle parameters $\chi_r, \gamma_r, \beta_r$ defined from reference line $\overline{OP}$ shown in Fig. 9.

Substituting $\chi = \pi/2 + \chi_r$, $\gamma = \pi/2 + \gamma_r$ and $\beta = \pi/2 + \beta_r$ into Eqs. (1)-(3) and (5), we obtain

$$\sin\gamma_r = \sin\alpha \sin\chi_r \tag{42}$$

$$\sin\phi = \frac{\tan\gamma_r}{\tan\chi_r} \tag{43}$$

$$\sin\beta_r = \frac{\tan\gamma_r}{\tan\alpha} \tag{44}$$

$$\psi_r = \psi_{rp} + \frac{\chi_r}{\cos\alpha} - \beta_r \tag{45}$$

$$\psi_{rp} = \frac{\pi}{2}\left(\frac{1-\cos\alpha}{\cos\alpha}\right). \tag{46}$$

Furthermore, the crown rack's tooth-profile curve is defined from Eqs. (15)-(18). Substituting $\pi/2 + \gamma_r$ and $\pi/2 - \alpha$ into γ and γ_b, respectively in Eqs. (15)-(18), we obtain

$$\overrightarrow{OA_r} = \xi \overrightarrow{n_A} \tag{47}$$

$$\overrightarrow{n_A} = \cos\gamma_r \sin\eta_r \overrightarrow{i_r} + \cos\gamma_r \cos\eta_r \overrightarrow{j_r} - \sin\gamma_r \overrightarrow{k_r} \tag{48}$$

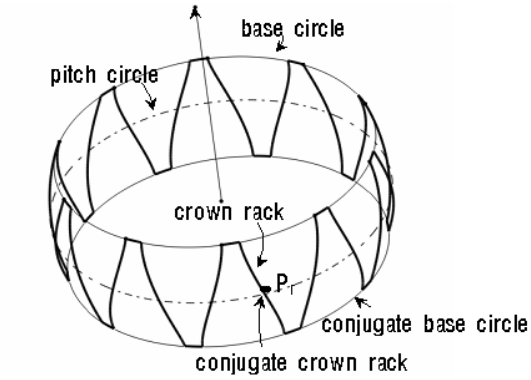

Fig. 10. Imaginary crown rack.

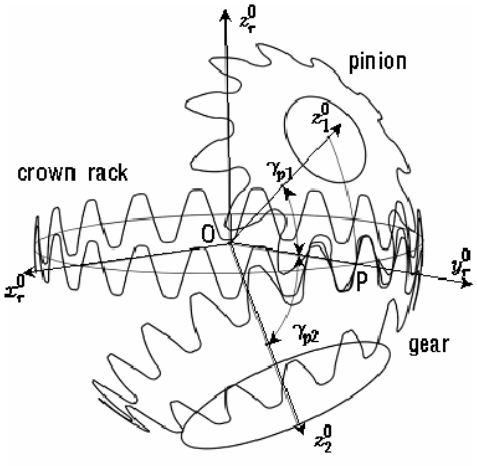

Fig. 11. Pinion and gear generated by a common crown rack.

$$\eta_r = \frac{1}{\cos o}\sin^{-1}\left(\frac{\sin\gamma_r}{\sin o}\right) - \sin^{-1}\left(\frac{\tan\gamma_r}{\tan o}\right). \quad (49)$$

In Eq. (49), η_r as a function of γ_r is the angle between $\widehat{C_rP_r}$ and $\widehat{C_rA_r}$, and $\eta_r(\gamma_r) = -\eta_r(-\gamma_r)$. Therefore, we find that the crown rack's tooth-profile curve $\widehat{D_rA_r}$ is point-symmetric with respect to the curve's center point P_r in Fig. 9. Accordingly, as shown in Fig. 10, the crown rack and its conjugate rack are of identical configuration, and the gear generated by the rack's front and rear sides is a homogeneous spherical involute gear.

In other words, the crown rack defined by Eqs. (42)-(44) or Eqs. (47)-(48) is a complete common basic rack of a spherical involute gear.

Fig. 11 shows a pinion and a gear with number of teeth $Z_1, Z_2 = 12,17$ generated by an imaginary crown rack of $m/\xi = 0.1$.

The pinion is generated by the crown rack's front side and the gear by the rear side (conjugate crown rack). There is a single point of contact between rack and pinion as well as between rack and gear. Since both gears maintain contact with the imaginary rack, the two gears have identical contact relationships at a common contact point. Therefore, we can verify that every gear generated by the same imaginary crown rack is compatible.

4. Consideration for bevel gear standardization

Although the spherical involute bevel gear-tooth profile has been theoretically published and displays exceptional performance and representative features, it has failed to become widely used presumably because its processing is difficult and manufacturing is costly. It is also a well-known fact that a more effective cutting technique can be developed based only on a solid theoretical foundation. Unlike spur gears, bevel gears were first distributed in the industry in the form of non-involute bevel gears. Bevel gear-tooth profiles that depended on expert machines mainly made by Gleason and Klingelnberg were very dissimilar to familiar involute tooth profiles, and the special gears were too difficult to understand. Their design and manufacturing processes are far more complex and difficult than those of spur and helical involute gears. Accordingly, it is an imperative task to expedite standardization of bevel gears so that the widely used spur and helical involute gear design approaches can be succeeded to solidify the theoretical foundation for bevel gears. Active theoretical studies will encourage development of more efficient cutting techniques. In the previous chapter, the geometrical superiority of a theoretically complete spherical involute gear was examined and a crown rack was mathematically established as a theoretically complete basic rack capable of generating spherical involute gears. It is hoped that more effective hobbing, milling and cutting techniques will be developed based on the common basic rack drawing. If so, spherical involute bevel gears that are unlike commercial bevel gears will become widely available in the industry. The spherical involute gears will be compatible, and their axis alignment errors will be less sensitive to velocity transmission rates. This chapter proposes the standard tooth profile of a complete crown rack capable of generating standard bevel gears. The tooth profile is developed by benchmarking the widely known linear rack tooth profile. If we can maintain the characteristics of the conventional spur involute gear and use a similar design approach, it will offer an optimal standard bevel gear model. The crown rack's standard tooth profile consists of an involute part, a round-tip part and an addendum/dedendum part. Specific dimensions are determined according to the methodology used in a linear rack [5]. The involute part should be positioned so that the height of the generated involute tooth surface is equal to module. The radius of the round-tip part is recommended to 0.3m. Considering the gap of the generated gear, the addendum/dedendum circle should be positioned so that the height of the tooth tip is 1.25m from the pitch circle. For the gap between the tooth tip of the cut gear and the tooth root of the crown rack to maintain 0.05m, the gear blank's tooth-tip height is set at 1.2m. (where m is a module.)

In Fig. 12, an arc $\widehat{A_{ah}A_{at}}$ with a cone angle of ρ is securely placed between the tooth profile circle and the adden-

Table 1. The tooth-tip height angle of the crown rack.

m/ξ	$\gamma_{ah}/(m/\xi)$	
	$\alpha = 14.5°$	$\alpha = 20°$
0.000	1.0251	1.0526
0.001	1.0251	1.0526
0.015	1.0250	1.0525
0.159	1.0232	1.0513
0.200	0.9985	1.0355

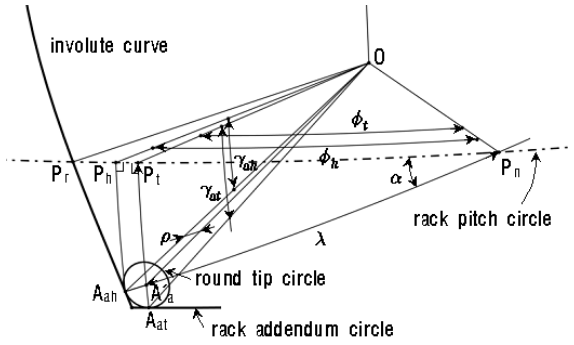

Fig. 12. Round tip circle of the crown rack.

dum circle.

The position of the cone's center point A_a' is obtained from the geometrical relationship of spherical triangle $\Delta A_a' P_t P_n$.

$$\cos\alpha = \frac{\tan\phi_t}{\tan\lambda} \tag{50}$$

$$\cos\lambda = \cos(\gamma_{at} - \eta)\cos\phi_t \tag{51}$$

Eliminating ϕ_t from Eqs. (49) and (50) gives

$$\sin\lambda = \frac{\sin(\gamma_{at} - \eta)}{\sin\alpha}. \tag{52}$$

From spherical triangle $\Delta A_{ah} P_h P_n$,

$$\cos\alpha = \frac{\tan\phi_h}{\tan(\lambda + \eta)} \tag{53}$$

$$\cos(\lambda + \eta) = \cos\gamma_{ah}\cos\phi_h. \tag{54}$$

Eliminating ϕ_h from the two equations gives

$$\sin\gamma_{ah} = \sin(\lambda + \eta)\sin\alpha. \tag{55}$$

Table 1 lists the calculation of the crown rack's tooth-tip height angle γ_{ah} for $\alpha = 14.5°, 20°$ and $m/\xi = 0.000 \sim 0.200$ from Eqs. (52) and (55).

The case of $m/\xi = 0.000$ represents a linear rack. The table indicates that $\gamma_{ah}/(m/\xi)$ converges toward 1.0, which means the active part of involute curve in the rack has a height about 1.0m. Accordingly, we can verify that the method using a round-tip radius of 0.3m and an addendum tooth height of 1.25m is very adequate for the crown rack.

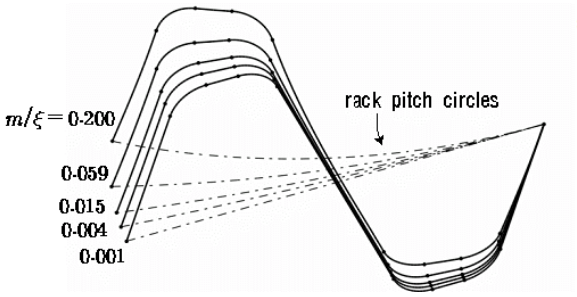

Fig. 13. Crown rack with respect to $\alpha = 20°$ and $m/\xi = 0.000 \sim 0.200$.

Fig. 13 depicts crown rack tooth-profile curves when $\alpha = 20°$ and $m/\xi = 0.000 \sim 0.200$

5. Generation of a proposed standard bevel gear

Specifications for a standard bevel gear generated with a crown rack of the standard tooth profile are determined according to the basic specifications of the crown rack. If the crown rack's basic specifications are given in terms of module, tool pressure angle and cone distance, the module and pitch of the generated gear are identical to those of the crown rack. If the number of gear teeth Z_g is given, the gear's pitch radius is $R_{sg} = mZ_g/2$ and the standard pitch-cone angle is

$$\gamma_{sg} = \sin^{-1}\left(\frac{mZ_g}{2\xi}\right). \tag{56}$$

From Eq. (9), the gear's base-cone angle γ_{bg} is

$$\gamma_{bg} = \sin^{-1}(\cos\alpha\sin\gamma_{sg}). \tag{57}$$

The standard bevel gear-tooth surface generated by a single cycle of crown rack-tooth surface is obtained from the equation of meshing. The gear mesh equation can be mathematically expressed as follows.

$$\vec{N} \bullet \overrightarrow{\Delta V} = 0 \tag{58}$$

$$\vec{N} = \frac{\partial \overrightarrow{OA_r}}{\partial \eta_r} \times \frac{\partial \overrightarrow{OA_r}}{\partial \xi} \tag{59}$$

$$\overrightarrow{\Delta V} = (\overrightarrow{\Omega_g} - \overrightarrow{\Omega_r}) \times \overrightarrow{OA_r} \tag{60}$$

where η_r and ξ are free parameters.

The crown rack-tooth surface $\overrightarrow{OA_r}$ is identically expressed with the Eqs. (47) and (48) where the cone angle γ_r encompasses not only the involute part but also every curve in the fillet, addendum and dedendum part. So γ_r is expressed with a general form as a function of η_r according to each

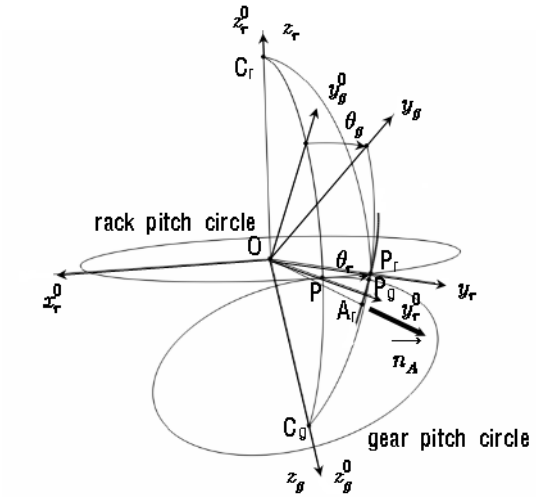

Fig. 14. Bevel gear generated by the crown rack cutter.

curve part.

$$\gamma_r = \gamma_r(\eta_r)\,. \tag{61}$$

Applying Eqs. (47), (48) and (61) to Eqs. (58)-(60), we obtain a single algebraic equation for parameter η_r and crown rack's rotational motion θ_r (Refer to Fig. 13)

$$f(\eta_r, \theta_r) = 0\,. \tag{62}$$

The gear-tooth profile curve is obtained by transforming Eq. (47) into the gear fixed coordinate system C_g. If we denote vector $\overrightarrow{OA_r}$'s C_g coordinate elements as x_g, y_g, z_g,

$$x_g = \overrightarrow{OA_r} \bullet \vec{i_g} \tag{63}$$

$$y_g = \overrightarrow{OA_r} \bullet \vec{j_g} \tag{64}$$

$$z_g = \overrightarrow{OA_r} \bullet \vec{k_g} \tag{65}$$

In Fig. 14, the crown rack fixed coordinate system C_r rotates around z_r axis by θ_r, and the gear fixed coordinate system C_g rotates around z_g axis by $-\theta_g$. Since the two pitch circles are in rolling-contact motion,

$$\theta_g = \frac{\theta_r}{\sin\gamma_p} \tag{66}$$

and $\vec{i_r}, \vec{i_g}, \cdots, \vec{k_r}, \vec{k_g}$ are represented as a function of θ_r, θ_g from the relationship between the two object fixed coordinate systems. Accordingly, x_g, y_g, z_g in Eqs. (63)-(65) are expressed as functions of variables η_r, ξ and θ_r, θ_g. Since θ_r, θ_g are transposed to η_r from Eqs. (62) and (66), x_g, y_g, z_g become functions of two free parameters η_r, ξ. Consequently, we were able to obtain a surface equation for the complete spherical involute gear generated by the crown rack, and subsequently the mathematical representations of all tooth-profile curves of involute, fillet, addendum and dedendum parts. Fig. 15 displays the crown rack and the tooth profile of the spherical involute gear it generates.

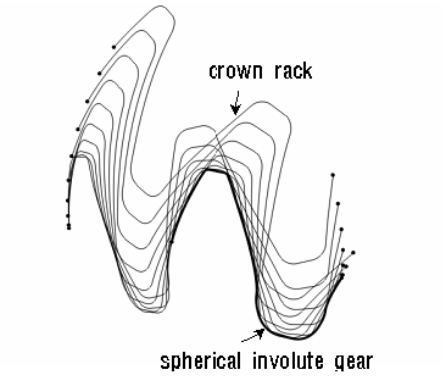

Fig. 15. Spherical involute gear generated by the crown rack ($m/\xi = 0.2, Z_g = 9$).

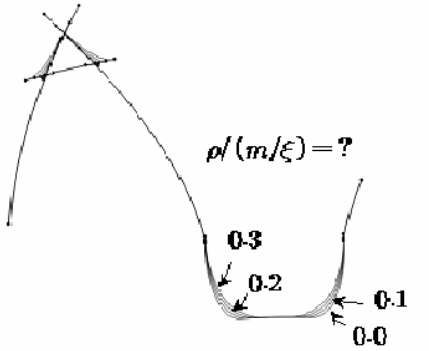

Fig. 16. Fillet curves along the radius of the round tip.

Fig. 16 exhibits the fillet part curve according to the round-tip radius of the crown rack with radius range 0~0.3m. The Fig. illustrates that the tooth thickness of the fillet part increases in proportion with the round-tip radius.

If the number of teeth of the gear to be generated is less than a certain threshold, undercut occurs. According to undercut prevention conditions specified by Litvin [4], the point where the gear's direction of velocity coincides with the direction of the circle of action's tangent line is the undercut threshold point. The undercut threshold point in a spherical involute gear system is the contact point between the base circle and the circle of action. Accordingly, undercut occurs if the crown rack's tooth cut curve tip A_{ah} shown in Fig. 11 is positioned higher than contact point B_g in Fig. 17.

Therefore, the bevel gear's threshold number of teeth is obtained by calculating the gear's pitch-circle radius when the tooth-tip point of a crown rack with module m passes through point B_g. From spherical triangles $\Delta C_g B_g P$ and $\Delta C_g E B_g$ in Fig. 17,

$$\cos\beta = \frac{\tan\gamma_b}{\tan\gamma_p} \tag{67}$$

Table 2. The threshold number of teeth for avoiding undercut.

γ_a(°)	Z_{cr}	
	$\alpha = 14.5°$	$\alpha = 20°$
0	32	17
10	31	17
20	30	16
30	28	15
40	25	13
50	21	11
60	16	9
70	11	6
80	6	3
90	2	2

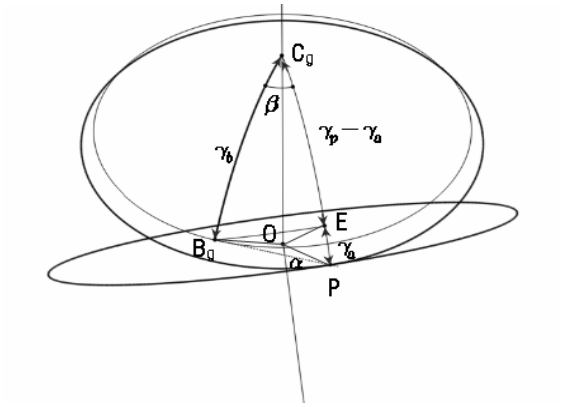

Fig. 17. Undercut in bevel gear system.

$$\cos\beta = \frac{\tan(\gamma_p - \gamma_a)}{\tan\gamma_b}. \tag{68}$$

Eliminating β, we have

$$\gamma_a = \tan^{-1}(\tan\gamma_p \sin^2\alpha) \tag{69}$$

and the condition to prevent undercut should be $\gamma_a \geq m/\xi$. However, from the relationship $m/\xi = 2\sin\gamma_p / Z$, the threshold number of teeth becomes

$$Z_{cr} = \frac{2\sin\gamma_p}{y_a}. \tag{70}$$

Table 2 lists the threshold numbers of teeth according to pitch-cone angle γ_a.

The threshold number of teeth increases as the pressure angle is reduced, and vice versa. It can be verified that with $\alpha = 20°$ and $\gamma_p -> 0$, the result is identical with the spur gear's threshold number of teeth 17. As γ_p increases to $\pi/2$, the threshold number of teeth decreases and becomes 2 when $\gamma_p -> \pi/2$ (crown rack). Fig. 18 displays the tooth-profile curve of an undercut gear.

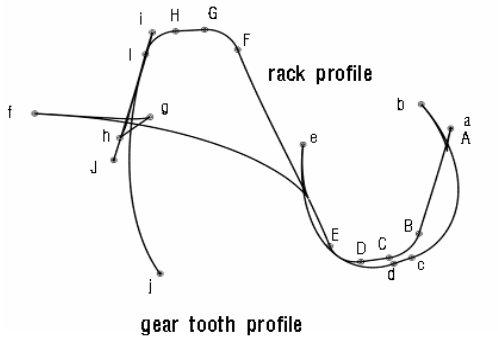

Fig. 18. Tooth profile with undercut ($m/\xi = 0.2, Z_g = 6, Z_{cr} = 9$).

6. Conclusions

This paper performed a comparative analysis of spherical involute gears—the most ideal of bevel gears—and widely known cylindrical involute gears to examine the similarities and differences in terms of their geometrical and kinematic properties. The spherical involute gear was proposed as a standard bevel gear model most appropriate for bevel gear systems, and corresponding proprieties were studied. Fillet curve characteristics and undercutting were examined for the proposed standard bevel gear, and it was confirmed that the findings were very similar to the properties of spur involute standard gears.

The common basic rack configuration is an essential element that must be established not only for understanding a gear's kinematic characteristics, but also for developing hobbing and milling techniques. This paper explained the bevel gear's common basic rack, which had not been established up to this point. The common basic rack was developed using the gear mesh equation from the spherical involute gears that have been published in theory. Since the rack and its conjugate rack have identical configurations, it is clear that the spherical involute crown rack driven in this paper is the common basic rack for bevel gear systems, which indicates that spherical involute bevel gears are truly compatible. Based on analysis, it was found that the tooth profile of the common basic rack is the tooth profile of a spherical involute gear with a pitch-cone angle of $\pi/2$ and a base-cone angle of $\pi/2-\alpha$.

Therefore, it is believed that spherical involute bevel gears are most qualified to be widely used as standard bevel gears. The author hopes that more fundamental and profound studies are conducted regarding spherical involute gears and innovations made in their processing techniques to become widely used throughout the industry and secure their position as standard bevel gears.

Nomenclature

B	:	Backlash
$C_g{}^0(x_g{}^0, y_g{}^0, z_g{}^0)$	:	Space fixed coordinate system
$C_g(x_g, y_g, z_g)$	:	Body fixed coordinate system
m	:	Module

$\vec{N}$: Normal vector at tooth contact point
$\overrightarrow{n_A}$: Direction vector at point A
t, t_p, t_b : Tooth thicknesses
$\overrightarrow{V_*^*}$: Velocity at point A_*^*
Z_{cr} : Threshold number of undercut
γ_a : Addendum cone angle
γ_{ah}, γ_{at} : Cone angles of tooth height and tip
ΔV : Velocity difference at tooth contact point
ρ : Round tip cone angle
λ : Contact normal angle
ξ : Cone distance
θ_g, θ_r : Rotating angles of gear and rack circle
ϕ_h, ϕ_t : Azimuth angles
$\Omega_r, \overrightarrow{\Omega_r}$: Magnitude and vector of crown rack rotational velocity
$\Omega_g, \overrightarrow{\Omega_g}$: Magnitude and vector of gear rotational velocity

References

[1] Y. C. Tsai and P. C. Chin, Surface Geometry of Straight and Spiral Bevel Gears, *Transactions of the ASME, Journal of Mechanisms, Transmissions, and Automation in Design*, 109 (1987) 443-449.

[2] W. D. Mark, The Generalized Transmission Error of Spiral Bevel Gear, *Journal of Mechanics, Transmissions, and Automation in Design,* 109 (1987) 275-282.

[3] M. J. Al-Daccak, J. Angels and M. A. Gonzles-Palacios, The Modeling of Bevel Gears Using the Exact Spherical Involute, *Transactions of the ASME, Journal of Mechanical Design*, 116 (1994),364-368.

[4] F. L. Litvin and A. Fuentes, Gear Geometry and Applied Theory, Second Edition, Cambridge University Press (2004) 98-99.

[5] J. R. Colbourne, The Geometry of Involute Gears, Springer-Verlag (1987) 137-138.

Appendix

A.1 Geometry of the spherical triangle

A line connecting two points on the surface of a reference sphere is an arc. The relationships in the triangle formed by connecting three points on a sphere surface will be different from those of a plane triangle. Fig. A.1 displays triangle $\Delta A_1B_2C_3$ on the surface of a sphere with center O and radius ξ. If we denote the tangent lines that contact arcs $\widehat{A_1B_1}$ and $\widehat{A_1C_3}$ at apex A_1 as $\overline{A_1B_1}$ and $\overline{A_1C_1}$, respectively, the following relationship holds for plane triangle $\Delta A_1B_1C_1$.

$$(\overline{B_1C_1})^2 = (\overline{A_1B_1})^2 + (\overline{A_1C_1})^2 - 2(\overline{A_1B_1})(\overline{A_1C_1})\cos\alpha \quad \text{(A1)}$$

In triangle ΔOB_1C_1,

$$(\overline{B_1C_1})^2 = (\overline{OB_1})^2 + (\overline{OC_1})^2 - 2(\overline{OB_1})(\overline{OC_1})\cos A \quad \text{(A2)}$$

and In ΔOA_1B_1 and ΔOA_1C_1,

$$\overline{A_1B_1} = \overline{OA_1}\tan\Gamma \quad \text{(A3)}$$

$$\overline{OB_1} = \overline{OA_1}/\cos\Gamma \quad \text{(A4)}$$

$$\overline{A_1C_1} = \overline{OA_1}\tan B \quad \text{(A5)}$$

$$\overline{OC_1} = \overline{OA_1}/\cos B\,. \quad \text{(A6)}$$

Substituting Eqs. (A2)-(A6) into Eq. (A1) and rearranging, we obtain

$$\cos A = \cos B\cos\Gamma + \sin B\sin\Gamma\cos\alpha \quad \text{(A7)}$$

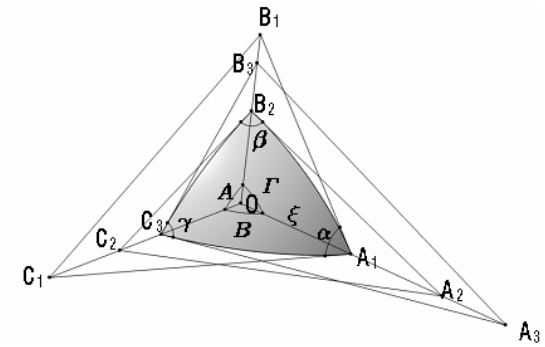

Fig. A.1. Spherical triangle and its relations.

Likewise, if we apply similar processes to plane triangles $\Delta A_2B_2C_2$ and $\Delta A_3B_3C_3$, we obtain the following relationships:

$$\cos B = \cos\Gamma\cos A + \sin\Gamma\sin A\cos\beta \quad \text{(A8)}$$

$$\cos\Gamma = \cos A\cos B + \sin A\sin B\cos\gamma \quad \text{(A9)}$$

If $\Delta A_1B_2C_3$ is a right spherical triangle with $\alpha = 90°$, from Eq. (A7)

$$\cos A = \cos B\cos\Gamma \quad \text{(A10)}$$

Eliminating B or A from Eqs. (A8) and (A10) and rearranging,

$$\tan\Gamma = \tan A\tan\beta \quad \text{(A11)}$$

$$\tan B = \tan\beta\sin\gamma \quad \text{(A12)}$$

Eliminating Γ from Eqs. (A9) and (A10), we obtain

$$\tan B = \tan A\cos\gamma \quad \text{(A13)}$$

Noh Gill Park received his B.S in Mechanical Engineering from Seoul National University, Korea in 1977. He is received a PH.D degree at North Carolina State University, USA in 1987. Prof. Park is currently a Professor of School of Mechanical Engineering of Pusan National University, Korea. His research fields are design technology of wind turbine gear train, involute hypoid gearing and CVT-joint development.

Hyoung Woo Lee received his B.S, M.S, and Ph.D in Mechanical Engineering from Pusan National University, Korea in 1991, 1994 and 1999, respectively. Prof. Lee is currently a Professor of Education Center for Green Industry-friendly Fusion Technology of Pusan National University, Korea. His research fields are design technology of wind turbine gear train, automotive transmission and special gear mechanism.